

Supplementary material

Coordinated signals from the DNA repair enzymes PARP-1 and PARP-2 promotes B-cell development and function

Miguel A. Galindo-Campos¹, Marie Bedora-Faure², Jordi Farrés¹, Chloé Lescale², Lucia Moreno-Lama¹, Carlos Martínez³, Juan Martín-Caballero⁴, Coral Ampurdanés¹, Pedro Aparicio⁵, Françoise Dantzer⁶, Andrea Cerutti^{7,8}, Ludovic Deriano^{2*}, José Yélamos^{1,9*}

Supplemental Figure legends

Figure S1.- B-cell specific deletion of PARP-2 in a PARP-1-deficient background results in defective lymph nodes B cells. Flow cytometry analysis of lymph nodes from 8 to 10-weeks old mice of the indicated genotype. (A) Representative dot-plots showing lymph node cells analyzed for the expression of the indicated markers. Percentage of cells in the individual subpopulations with regard to each gate is indicated in each quadrant. (B) Bars represent the percentage of lymph node B lymphocytes for the indicated genotype. Values represent the mean \pm SEM of at least 4 mice of each genotype. *P < 0.05.

Figure S2.- Effectiveness of PARP-2 deletion in marginal zone and follicular B cells from Cd19-cre;Parp-2^{f/f} mice. PCR analysis from genomic DNA in sorted T cells, marginal zone (MZ) and follicular (FO) splenic cells from mice of the indicated genotypes.

Figure S3. Parp2 genotyping of v-abl pro-B cell lines

Figure S4. Igk rearrangements in v-abl pro-B cell lines. PCR analysis of Vk6-23/Jk1 coding joints (upper panel) and Vk10-95/Jk4 coding joints (middle panel) from indicated v-abl pro-B cell lines untreated (-) and treated for 72h (+) with ABLki. Il-2 gene PCR (bottom panel) was used as a loading control.

Figure S5.- 53BP1 DNA damage response foci in *v-abl* pro-B-cell lines. (A) Representative 3D projections of 53BP1 immuno-staining conducted on ABLki-treated *v-abl* pro-B-cells. Nuclei were stained with anti-53BP1 antibody (green) and DAPI. Cells were imaged in 3D (9 Z stacks of 0.5 μm) using a Zeiss AxioImager Z2 microscope (x40 objective) and the Metacyte automated capture system (Metasystems), (B) Percentage of *v-abl* pro-B-cells of the indicated genotype harboring 1 or 2 53BP1 foci 65h post-ABLki treatment (See Table S3 for details).

Figure S6.- PARP-1/PARP-2 doubly deficiency in B-cells did not alter basal immunoglobulin levels. Total levels of IgM, IgG1, IgG2a, IgG2b and IgG3 were assessed in the sera of 6-8-weeks old mice of the indicated genotypes by ELISA. Dots represent individual mice and horizontal lines represent median values.

Figure S7.- PARP-1/PARP-2 doubly deficiency in B-cells did not alter the percentage of germinal center B cells in Peyer's patches. (A) Representative dot-plots of B220⁺ B lymphocytes in Peyer's patches isolated from 10-12 weeks-old mice of the indicated genotypes. Percentage of Germinal centres (GC) B cells (GL7⁺CD95⁺) cells is indicated. (B) Graph showing the percentage of GC in Peyer's patches. Values represent the mean \pm SEM of 5 mice of each genotype.

Supplemental Table legends

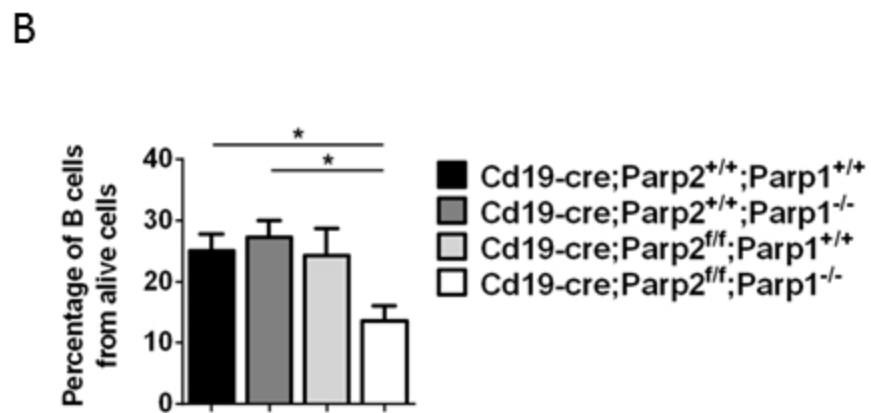
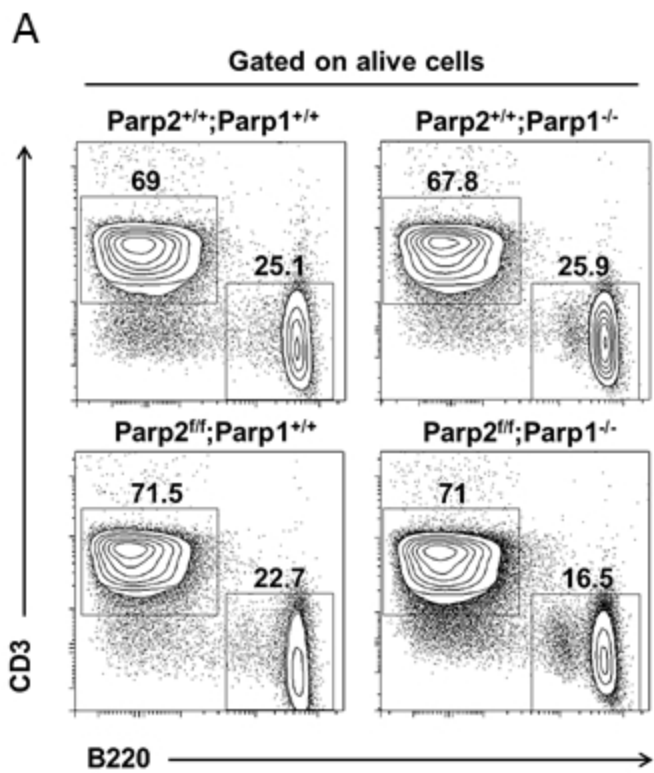
Table S1.- Renewal and production rates of bone marrow B cell subsets determined by in vivo BrdU labeling. The percentage of BrdU-labeled bone marrow B cell subsets was determined by flow cytometry and the number of BrdU-labeled cells was calculated by multiplying the percentage BrdU⁺-cells of each population by the total number of cells in that population. The regression coefficients of proportional and absolute BrdU labeling versus time provide estimations of renewal and production, respectively. *P < 0.05; **P < 0.001.

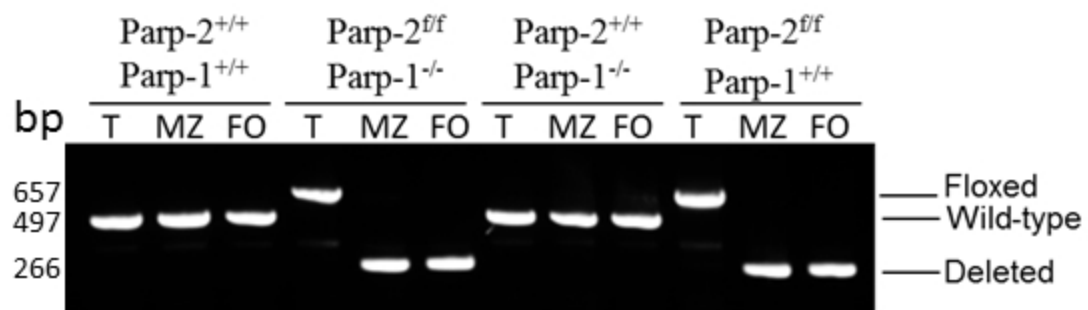
Table S2.- List and origin of *v-abl* pro-B-cell lines

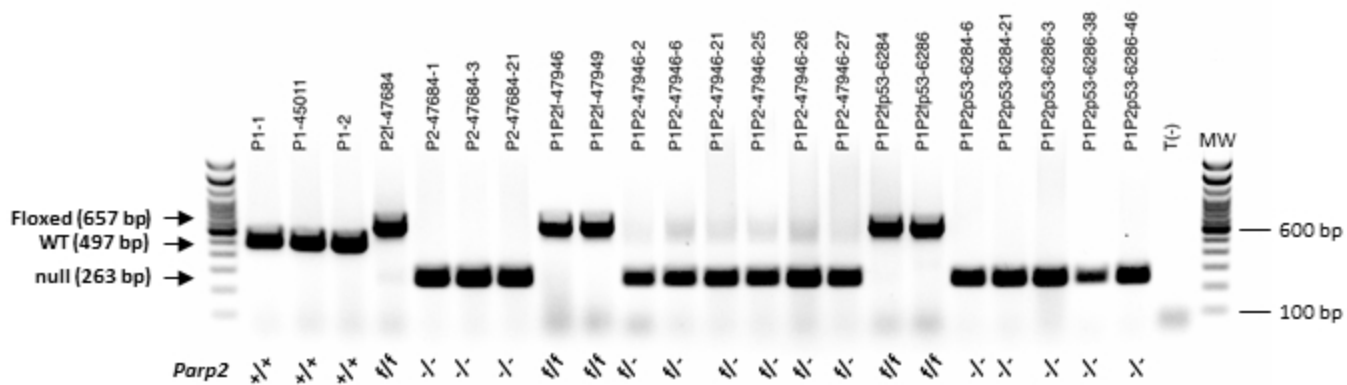
Table S3.- 53BP1 DNA damage response foci after RAG induction. Number and percentage of *v-abl* pro-B-cells harboring 0, 1, 2 or >2 53BP1 foci 65 hours after ABLki

treatment.

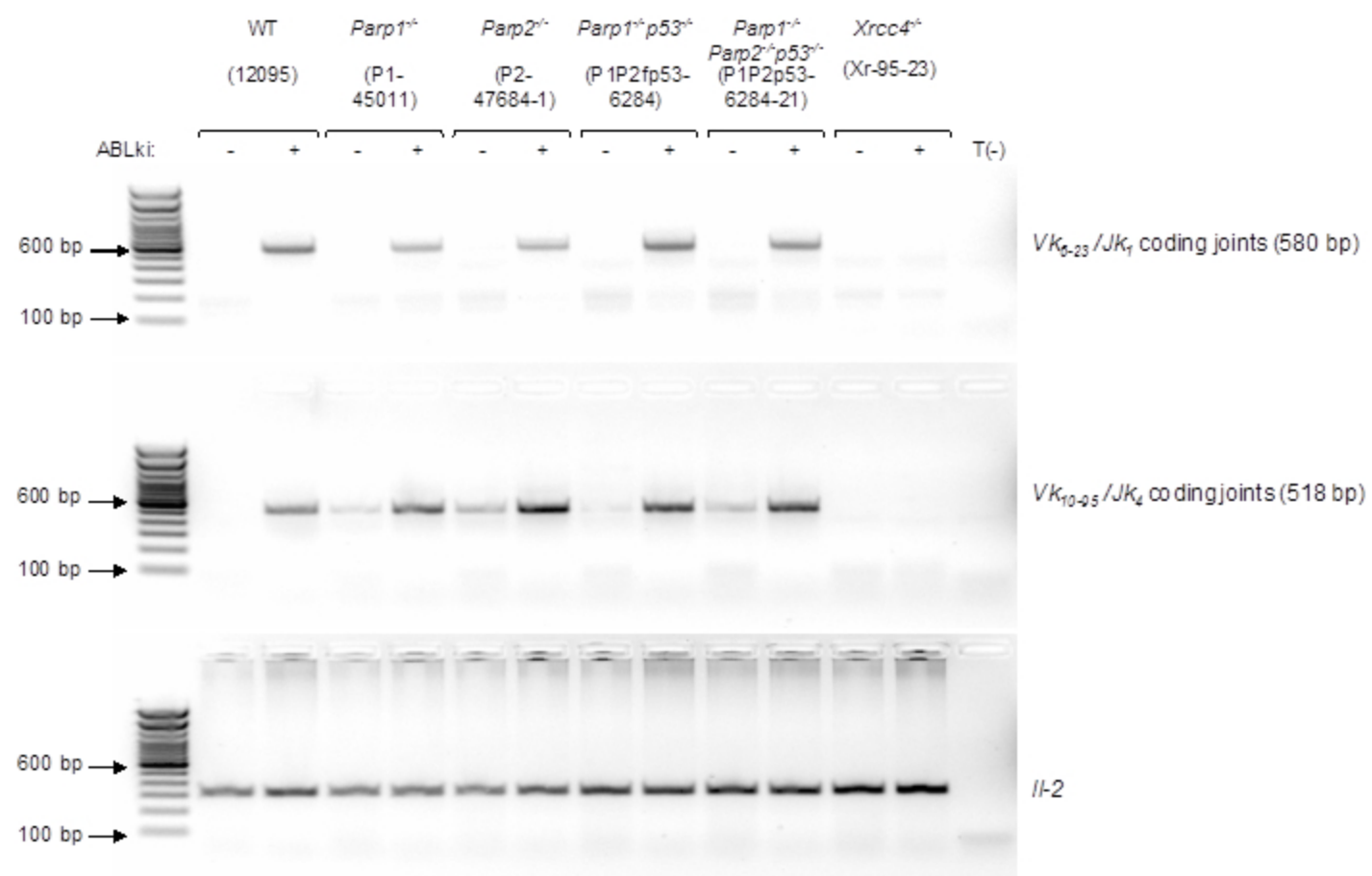
Table S4. Genomic instability at the *Igk* locus in *v-abl* pro-B-cells. Number and percentage of aberrant metaphases harboring chromosome breaks and/or translocations involving the *Igk* locus from untreated and ABLki-treated and released (shown in Figure 3E and F) *v-abl* pro-B-cell lines of the indicated genotypes are indicated. DNA FISH experiments were performed using probes centromeric (*Igk V*) and telomeric (*Igk C*) to the *Igk* locus plus specific paint for chromosome 6.





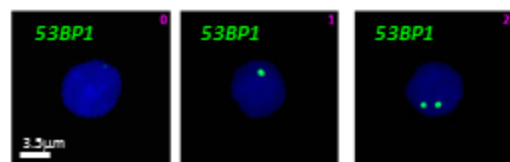


Galindo-Campos et al., Fig. S3

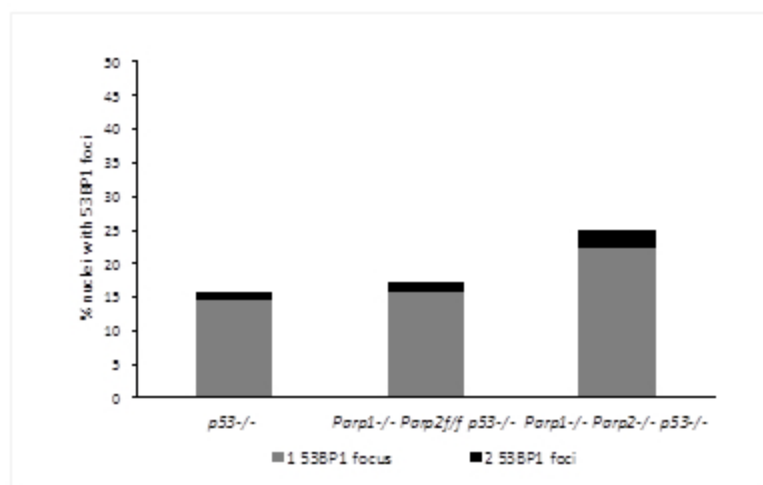


Galindo-Campos et al., Fig. S4

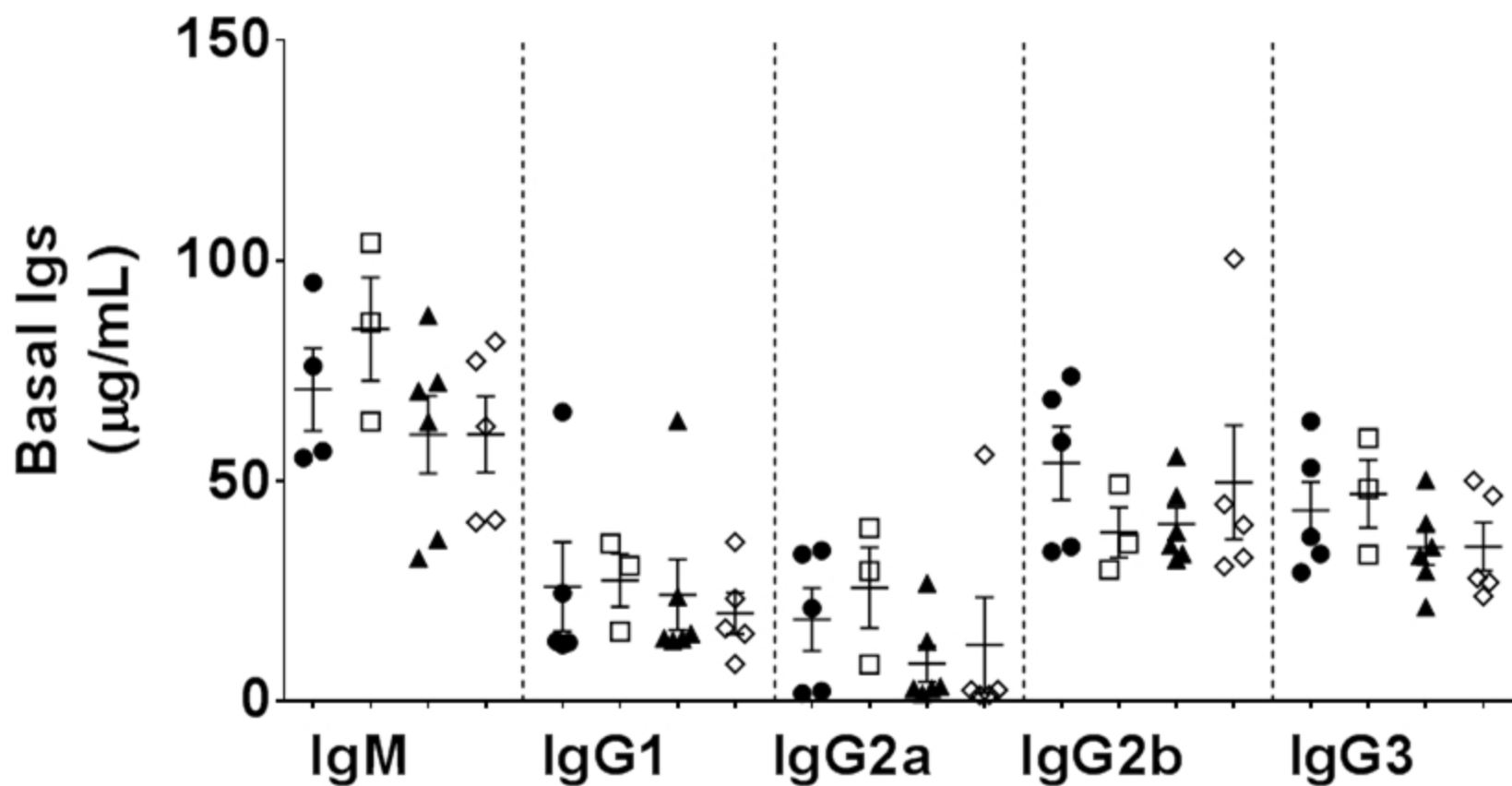
A



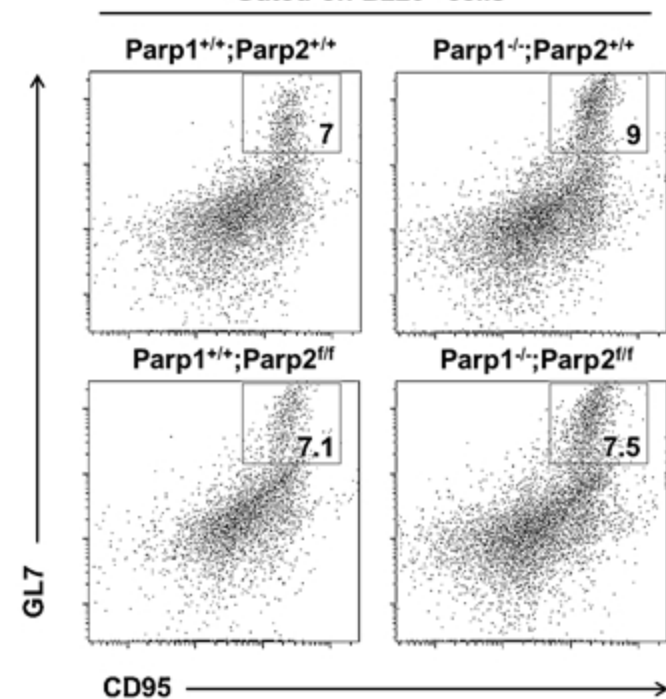
B



- Cd19-cre;Parp2^{+/+};Parp1^{+/+}
- Cd19-cre;Parp2^{+/+};Parp1^{-/-}
- ▲ Cd19-cre;Parp2^{f/f};Parp1^{+/+}
- ◇ Cd19-cre;Parp2^{f/f};Parp1^{-/-}



A

Gated on B220⁺ cells

B

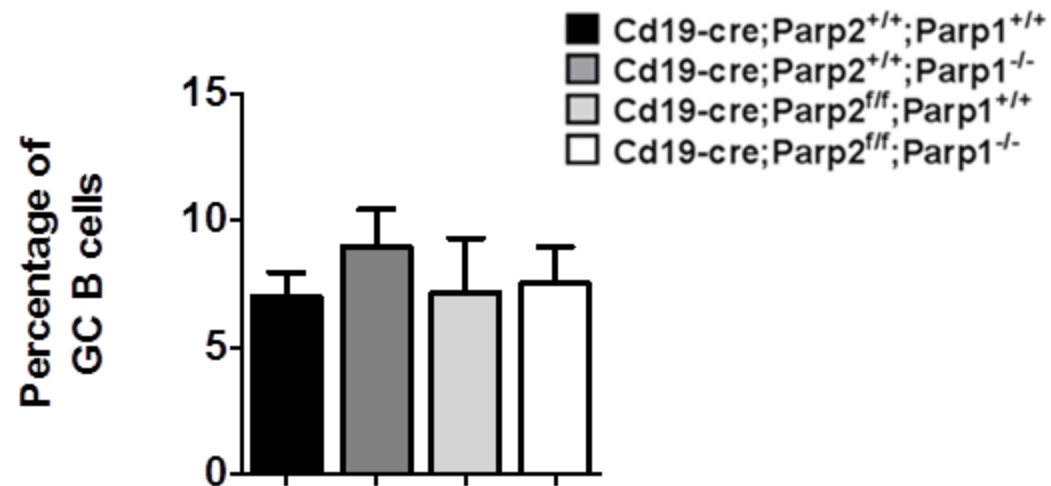


Table S1.- Renewal and production rates of bone marrow B cell subsets determined by in vivo BrdU labeling.

		Cd19-cre			
		Parp2^{+/+}; Parp1^{+/+}	Parp2^{+/+}; Parp1^{-/-}	Parp2^{fl/fl}; Parp1^{+/+}	Parp2^{fl/fl}; Parp1^{-/-}
Fraction A-C'	Renewal rate (% of pool/day)	33.29	34.29	34.66	34.87
	Production rate (cells/day X10 ⁶)	0.64	0.57	0.55	0.55
Fraction D	Renewal rate (% of pool/day)	39.80	39.69	38.75	39.62
	Production rate (cells/day X10 ⁶)	2.44	2.27	2.21	0.95 ***
Fraction E	Renewal rate (% of pool/day)	26.72	24.08	23.73	26.91
	Production rate (cells/day X10 ⁶)	0.89	0.79	0.86	0.52*

*P < 0.05; ***P < 0.001

Table S2. List and origin of *v-abl* pro-B cell lines

Genotype	Cell line	Generation method	Origin
WT	WT-47947	<i>v-Abl/Bcl2</i> immortalization of bone marrow pro-B cells	Mouse
	WT-1	<i>v-Abl/Bcl2</i> immortalization of bone marrow pro-B cells	Mouse
	WT-47947-4	Cell clone	WT-47947
	12095	<i>v-Abl/Bcl2</i> immortalization of bone marrow pro-B cells	Mouse
<i>Parp2^{fl/fl}</i>	P2f-47684	<i>v-Abl/Bcl2</i> immortalization of bone marrow pro-B cells	Mouse
<i>Parp2^{-/-}</i>	P2-47684-1	Cre infection	P2f-47684
	P2-47684-3	Cre infection	P2f-47684
	P2-47684-21	Cre infection	P2f-47684
<i>Parp1^{-/-}</i>	P1-1	<i>v-Abl/Bcl2</i> immortalization of bone marrow pro-B cells	Mouse
	P1-45011	<i>v-Abl/Bcl2</i> immortalization of bone marrow pro-B cells	Mouse
	P1-2	Cell clone	JYL-Pa1
<i>Parp1^{-/-} Parp2^{fl/fl}</i>	P1P2f-47946	<i>v-Abl/Bcl2</i> immortalization of bone marrow pro-B cells	Mouse
	P1P2f-47949	<i>v-Abl/Bcl2</i> immortalization of bone marrow pro-B cells	Mouse
<i>Parp1^{-/-} Parp2^{fl/fl}</i>	P1P2-47946-2	Cre infection	P1P2f-47946
	P1P2-47946-6	Cre infection	P1P2f-47946
	P1P2-47946-21	Cre infection	P1P2f-47946
	P1P2-47946-25	Cre infection	P1P2f-47946
	P1P2-47946-26	Cre infection	P1P2f-47946
	P1P2-47946-27	Cre infection	P1P2f-47946
<i>Parp1^{-/-} Parp2^{fl/fl} p53^{-/-}</i>	P1P2fp53-6284	<i>v-Abl/Bcl2</i> immortalization of bone marrow pro-B cells	Mouse
	P1P2fp53-6286	<i>v-Abl/Bcl2</i> immortalization of bone marrow pro-B cells	Mouse
<i>Parp1^{-/-} Parp2^{-/-} p53^{-/-}</i>	P1P2p53-6284-6	Cre infection	P1P2fp53-6284
	P1P2p53-6284-21	Cre infection	P1P2fp53-6284
	P1P2p53-6286-3	Cre infection	P1P2fp53-6286
	P1P2p53-6286-38	Cre infection	P1P2fp53-6286
	P1P2p53-6286-46	cre infection	P1P2fp53-6286
<i>p53^{-/-}</i>	15307	<i>v-Abl/Bcl2</i> immortalization of bone marrow pro-B cells	Mouse
<i>Xrcc4^{-/-}</i>	Xr-95-23	CRISPR/Cas9 editing	12095

Table S3. 53BP1 DDR foci after RAG induction. Related to Figure 3.

Number and percentage of *v-abl* pro-B cells harboring 0, 1, 2 or >2 53BP1 foci 65 hours after ABLki treatment.

	p53 ^{-/-}			Parp1 ^{-/-} Parp2 ^{f/f} p53 ^{-/-}			Parp1 ^{-/-} Parp2 ^{-/-} p53 ^{-/-}		
	15307			6284			6284-6		
Cell line #1	Nb of 53BP1 foci/nuclei	Nuclei Nb	Nuclei %	Nb of 53BP1 foci/nuclei	Nuclei Nb	Nuclei %	Nb of 53BP1 foci/nuclei	Nuclei Nb	Nuclei %
	0	3926	83,9	0	4199	83,9	0	3033	82,1
	1	687	14,7	1	750	15	1	532	14,4
	2	56	1,2	2	48	1	2	92	2,5
	>2	11	0,2	>2	8	0,1	>2	36	1,1
	TOTAL	4680	100	TOTAL	5005	100	TOTAL	3693	100
Cell line #2				6286			6284-21		
	Nb of 53BP1 foci/nuclei	Nuclei Nb	Nuclei %	Nb of 53BP1 foci/nuclei	Nuclei Nb	Nuclei %	Nb of 53BP1 foci/nuclei	Nuclei Nb	Nuclei %
	0	4098	81,6	0	3735	74,6	0	3735	74,6
	1	832	16,6	1	1121	22,4	1	1121	22,4
	2	74	1,5	2	126	2,5	2	126	2,5
	>2	16	0,2	>2	22	0,5	>2	22	0,5
	TOTAL	5020	100	TOTAL	5004	100	TOTAL	5004	100
Cell line #3				6286-38					
	Nb of 53BP1 foci/nuclei	Nuclei Nb	Nuclei %	Nb of 53BP1 foci/nuclei	Nuclei Nb	Nuclei %	Nb of 53BP1 foci/nuclei	Nuclei Nb	Nuclei %
	0	1768	62	0	1768	62	0	1768	62
	1	903	31,7	1	903	31,7	1	903	31,7
	2	141	4,9	2	141	4,9	2	141	4,9
	>2	40	1,4	>2	40	1,4	>2	40	1,4
	TOTAL	2852	100	TOTAL	2852	100	TOTAL	2852	100
Cell line #4				6286-46					
	Nb of 53BP1 foci/nuclei	Nuclei Nb	Nuclei %	Nb of 53BP1 foci/nuclei	Nuclei Nb	Nuclei %	Nb of 53BP1 foci/nuclei	Nuclei Nb	Nuclei %
	0	3634	77,1	0	3634	77,1	0	3634	77,1
	1	945	20,1	1	945	20,1	1	945	20,1
	2	94	2	2	94	2	2	94	2
	>2	38	0,7	>2	38	0,7	>2	38	0,7
	TOTAL	4711	100	TOTAL	4711	100	TOTAL	4711	100

Table S4. Genomic instability at the *Igk* locus in *v-abl* pro-B cells. (Related to Figure 3)

Number and percentage of aberrant metaphases harboring chromosome breaks and/or translocations involving the *Igk* locus from untreated and ABLki-treated and released (shown in Figure 3E and F) *v-abl* pro-B cell lines of the indicated genotypes are indicated. DNA FISH experiments were performed using probes centromeric (*Igk V*) and telomeric (*Igk C*) to the *Igk* locus plus specific paint for chromosome 6.

		Untreated					
Genotype	Cell line #	Metaphases with <i>Igk</i> chromosome breaks	Metaphases with <i>Igk</i> translocations	Total aberrant metaphases	Total normal metaphases	Total metaphases analyzed	% aberrant metaphases
<i>p53</i> ^{-/-}	15307	0	0	0	120	120	0
	Pa1Pa2fp53-6284	0	0	0	105	105	0
	Pa1Pa2fp53-6286	0	0	0	183	183	0
	TOTAL	0	0	0	288	288	0
<i>Parp1</i> ^{-/-} <i>Parp2</i> ^{fl/fl} <i>p53</i> ^{-/-}	Pa1Pa2p53-6284-6	2	0	2	98	100	2
	Pa1Pa2p53-6284-21	0	0	0	100	100	0
	Pa1Pa2p53-6284-30	0	0	0	100	100	0
	Pa1Pa2p53-6286-38	0	0	0	100	100	0
	Pa1Pa2p53-6286-46	0	0	0	100	100	0
	TOTAL	2	0	2	498	500	0,4

		ABLki treated and released					
Genotype	Cell line #	Metaphases with <i>Igk</i> chromosome breaks	Metaphases with <i>Igk</i> translocations	Total aberrant metaphases	Total normal metaphases	Total metaphases analyzed	% aberrant metaphases
<i>p53</i> ^{-/-}	15307	0	3	3	98	101	3
	Pa1Pa2fp53-6284	0	1	1	104	105	0,9
	Pa1Pa2fp53-6286	0	4	4	96	100	4
	TOTAL	0	5	5	200	205	2,4
<i>Parp1</i> ^{-/-} <i>Parp2</i> ^{-/-} <i>p53</i> ^{-/-}	Pa1Pa2p53-6284-6	0	3	3	95	98	3,1
	Pa1Pa2p53-6284-21	0	2	2	98	100	2
	Pa1Pa2p53-6284-30	1	3	4	97	101	4
	Pa1Pa2p53-6286-38	0	3	3	97	100	3
	Pa1Pa2p53-6286-46	2	0	2	98	100	2
	TOTAL	3	11	14	485	499	3

Statistical analysis (Fisher exact test)		p value	Level
<i>p53</i> ^{-/-}	vs <i>Parp1</i> ^{-/-} <i>Parp2</i> ^{fl/fl} <i>p53</i> ^{-/-}	0,7	n.s
	vs <i>Parp1</i> ^{-/-} <i>Parp2</i> ^{-/-} <i>p53</i> ^{-/-}	1	n.s
<i>Parp1</i> ^{-/-} <i>Parp2</i> ^{fl/fl} <i>p53</i> ^{-/-}	vs <i>Parp1</i> ^{-/-} <i>Parp2</i> ^{-/-} <i>p53</i> ^{-/-}	1	n.s